











Damping Temperature Fluctuations in the EC155 Intake Tube

Steve Sargent, Campbell Scientific®, Inc.

Introduction

The eddy-covariance (EC) technique is widely used to quantify the exchange of heat, carbon dioxide, water vapor, and other trace gases between Earth's surface and the atmosphere.^a These data provide the information required to analyze carbon storage properties of various ecosystems, create accurate gas exchange budgets, and compare emissions characteristics between various land use such as agricultural lands, forestlands, sagebrush steppe, or urban plots and landfills.

The EC technique requires the measurement of vertical wind speed and a scalar of interest, such as CO₂ or H₂O. Ideally, these measurements would have low noise and high frequency response, and they would be colocated and synchronized. Wind velocity is typically measured with a three-dimensional ultrasonic anemometer, such as Campbell Scientific's CSAT3. CO₂ and H₂O are typically measured with an infrared gas analyzer, commonly abbreviated to IRGA, of which there are two basic types: open path and closed path. Campbell Scientific manufactures three different IRGAs: two open path, the EC150 and the IRGASON; and one closed path, the EC155. All are designed specifically for EC flux measurements. Each of these analyzers has distinct advantages and disadvantages which are described in the white paper, EC150, IRGASON, or EC155: Which CO, and H,O Eddy-Covariance System is Best for my Application.^b

Open-path IRGAs such as the IRGASON and the EC150 measure the density of CO₃ and H₃O in the measurement path. In openpath systems, fluctuations in temperature will cause fluctuations in CO, and H,O density, as temperature affects the density of air. Therefore, a sensible heat flux will cause an open-path EC system to measure an apparent CO₃ and H₃O flux. Similarly, because a latent heat (water vapor) flux causes the air to be diluted with H₂O, a latent heat flux gives rise to an apparent CO₂ flux. These effects are well known and gave rise to the Webb, Pearman, Leuning (WPL) corrections.^c These corrections can be significant for open-path EC systems.

Traditional closed-path IRGAs do not require WPL corrections.^d The temperature fluctuations are damped in the intake tube as the air sample is brought to the temperature of the sample cell. The water vapor is measured and accounted for on a point-by-point basis, allowing the closed-path IRGA to report CO, and H₂O as mixing ratios, or moles of CO, or H₂O, per mole of dry air. Most closed-path analyzers require more power than an open-path analyzer due to the power required for a pump to move the air sample through the sample cell. They often require shelter from the environment, which means the sample tube must be relatively long. The long tube degrades frequency response, especially for water vapor, and this degradation in water frequency response depends on relative humidity.

Two modern closed-path analyzers, the LI-7200 (LI-COR®) and the EC155 (Campbell Scientific®, Inc.) are designed specifically for eddy covariance. They are environmentally rugged to allow them to be mounted close to the sonic anemometer without an additional bulky shelter. They use very short intake tubes to help preserve frequency response, even with low-power pumps to move the air sample through the sample cell. The LI-7200 is normally used with a flow module (7200-101, LI-COR®, Inc.), while the EC155 is included as part of a complete eddy-covariance system (CPEC200, Campbell Scientific®, Inc.) The power consumption for the CPEC200 system is approximately 12 W, less than half the power consumption of the LI-7200 and its flow module.

^ahttp://fluxnet.ornl.gov/. Accessed 12/4/2014

^bSargent, S. 2012. "EC150, IRGASON, or EC155: Which CO₃ and H₃O Eddy-Covariance System Is Best for my Application." http://s.campbellsci.com/documents/us/technical-papers/ec_sensor_selection_guide.pdf

Webb, E.K., Pearman, G.J., and Leuning, R. 1980. "Correction of Flux Measurement for Density Effects due to Heat and Water Vapor Transfer." Quart. J. Roy. Meteor. Soc., 106, 85-100.

^dLeuning, R., Judd, M.J. 1996. "The relative merits of open- and closed-path analysers for measurement of eddy fluxes." Global Change Biol., 2, 241-253. eMammarella, I., Launianinen, S., Gronholm, T., Keronen, P., Pumpanen, J., Rannik, Ü., and Vesala, T. 2009. "Relative Humidity Effect on the High-Frequency Attenuation of Water Vapor Flux Measured by a Closed-Path Eddy Covariance System." J. Atmos. Ocean Tech., 26, 1856-1866.

Table 1 compares these two systems.

Model	Cell Volume (ml)	Flow (LPM)	Cell Residence Time (ms)	System Power (W) **	Calibration	Air Temperature Measurement
LI-7200	16	16*	64	27	Density	Two fine-wire thermocouples in the air stream
EC155	5.9	7	50	12	Mixing ratio	One rugged thermocouple in sample cell block

^{*}LI-7200 controls mass flow. Cell residence time is based on sea level.

TABLE 1: Comparison of two modern closed-path infrared gas analyzers

Although similar in many ways, these two IRGAs employ different strategies for the WPL temperature term. With the LI-7200, the user must trade water frequency response for temperature damping in designing an appropriate intake tube.^f As temperature fluctuations may not be sufficiently damped in the LI-7200 intake tube, this IRGA includes a fine-wire thermocouple at the inlet of the sample cell to measure the temperature of the air as it enters the sample cell. Because air temperature fluctuations are further damped as the air flows through the sample cell, the LI-7200 includes a second fine-wire thermocouple to measure the temperature of the air as it exits the sample cell. These thermocouples are designed to be replaced in the field when they fail. The LI-7200 is calibrated for number density, but it can calculate a dry mole fraction from the density using a weighted average of the two thermocouples. Alternately, the user may calculate fluxes with the native CO₂ and H₂O density measurements, and then calculate and apply WPL correction terms.^g

The EC155 takes a very different approach to the problem of air temperature fluctuations. The EC155 has a fully integrated intake tube assembly, making it unnecessary for the user to choose between water frequency response and temperature damping. This intake assembly is very light, compact, and aerodynamic, and is heated to reduce the risk of condensation and to help maintain water frequency response. The intake assembly is engineered both to preserve water frequency response^h and to damp temperature fluctuations to a negligible level before the air sample reaches the sample cell. The air sample is brought to the temperature of the sample cell, and the temperature of the sample cell is measured by a robust sensor embedded in the sample cell. This eliminates a point of failure by avoiding the use of fragile fast-response thermocouples in the air stream. The EC155 is calibrated directly for mixing ratios (not density) of CO₂ and H₂O, making it unnecessary for the user to calculate the WPL terms.

The very small size of the EC155 intake tube suggests it is important to verify its ability to damp temperature fluctuations. Rannick, et al. used a semi empirical model to give a conservative upper bound for the minimum length of tubing required to damp temperature fluctuations to a negligible level. This length is 1000 times the inner diameter, and damps the steady state to within 1%, regardless of the Reynolds number inside and outside the tube, and the tube heat transport coefficient. The EC155 intake tube is 58.4 cm (23.0 in) long and 2.67 mm (0.105 in) inner diameter, giving a length/diameter ratio of 220, much lower than the 1000 given by Rannik. However, this is a conservative bound based on the steady-state solution, and as Rannik points out, "... in reality fluctuations tend to dampen more vigorously due to...heat capacity of tube material." Rannik continues: "...the real damping distance along the tube remains to be determined experimentally in the future." This paper describes a laboratory technique to measure the attenuation of temperature fluctuations in an intake tube. This technique gives the attenuation as a spectral quantity, because the attenuation is strongly dependent on frequency. It gives the attenuation as a complex quantity (amplitude and phase), because the phase response has a significant effect on the residual WPL temperature term.

Methods

The attenuation of temperature fluctuations in the EC155 intake tube was measured in a laboratory experiment. The IRGA, its intake tube, and datalogger were part of a CPEC200 system (Campbell Scientific®, Inc.). This system includes a pump module controlled to pull 7 LPM of ambient air through the IRGA. Several additional thermocouples were attached at the intake tube, the sample cell, and the sample cell block. The standard CPEC200 datalogger program was modified to measure the additional thermocouples and to control power to a heat gun. It sampled at the normal 10 Hz, but performed a block average and saved the results at 2 Hz.

^{**}LI-7200: 12 W for the IRGA and 15 W for the flow module. EC155: 12 W for complete CPEC200 system.

Burba, G.G., McDermitt, D.K., Anderson, D.J., Furtaw, M.D., and Eckles, R.D. 2010. "Novel design of an enclosed CO₂/H₂O gas analyser for eddy covariance flux measurements." *Tellus*, *62B*, 743-748.

⁹Burba, G., Schmidt, A., Scott, R.L., Nakai, T., Kathilankal, J., Fratini, G., Hanson, C., Law, B., McDermitt, D.K., Eckles, R., Furta, M., and Velgersdyk, M. 2012. "Calculating CO₂ and H₂O eddy covariance fluxes from an enclosed gas analyzer using an instantaneous mixing ratio." *Global Change Biology*, *18*, 385-399.
^hSargent, S. 2012. Quantifying Frequency Response of Low-power, Closed-path CO₂ and H₂O Eddy-covariance System.
https://s.campbellsci.com/documents/us/technical-papers/cpec200 frequency response.pdf

Rannik, Ü., Vesala, T., and Keskinen, R. 1997. "On the damping of temperature fluctuations in a circular tube relevant to the eddy covariance measurement technique." *J. Geophys. Res.,* **102**, Issue D11, 12789-12794.

Two thermocouples were placed at the inlet of the EC155 intake tube. The first was a fast-response type E thermocouple with 0.0127 mm (0.0005 in) diameter wire (FW05, Campbell Scientific®, Inc.). The second was a type E thermocouple made with 0.127 mm (0.005 in) diameter wire mounted in a #10-32 fitting. A third thermocouple, identical to this one, was installed in the EC155 sample cell with its junction at the center of the sample cell, in the sample air stream. This pair of matched thermocouples measured the temperature fluctuations in the inlet and in the sample cell with frequency response sufficient for this experiment. The FW05 characterized the frequency response of its paired thermocouple. An additional thermocouple was attached to the sample cell block.

A heat gun (HL1802E, Steinel®) was aimed at the inlet, with its power connection controlled by the CPEC200's datalogger (CR3000, Campbell Scientific®, Inc.) by way of a solid-state relay (S505-0SJ625-000, Continental Industries, Inc., Mesa AZ). A separate fan blew ambient air onto the inlet from the side opposite the heat gun. This prevented ambient air, warmed by the nearby heat gun (powered off but still hot), from entering the inlet. The datalogger was programmed to cycle the heat gun on and off, first 1 s on and 1 s off, for 4096 s (~68 min), then doubled the on and off times until the period was 2048 s (34 min). Ambient air temperature was approximately 23 °C. The heat gun warmed the air to approximately 130 °C.

Data were processed using DADiSP® (DSP Development Corporation) to extract each segment corresponding to a different on/off interval, calculate a Fast Fourier Transform (FFT) for each thermocouple, and extract the amplitude and phase of the FFT at the excitation frequency. At each frequency, the amplitude of the temperature damping ratio was calculated as the ratio of the matched thermocouples, and the phase was calculated as their difference.

Results

The resulting time series for three example periods are shown in Figure 1 (2048 s, top; 128 s, middle; and 8 s, bottom). Figure 1 shows ensemble averages with mean subtracted. Cell air, cell block, and error data have been scaled as indicated in the legends

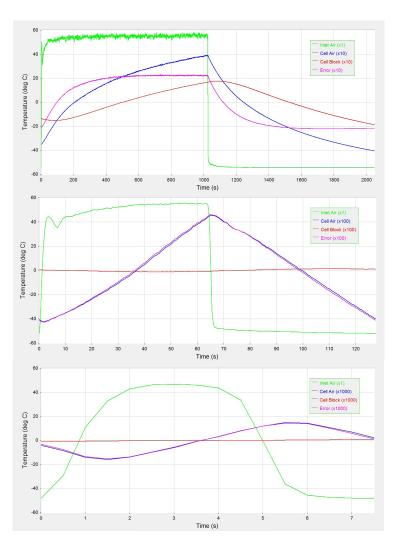


Figure 1. Example temperature time series for heat gun switching periods of 2048 s (top), 128 s (middle), and 8 s (bottom). Ensemble averages with means subtracted.

to allow comparison to the inlet air temperature. The top panel shows the inlet air temperature is nearly a square wave with an amplitude of approximately ±55 °C. The cell air temperature rises relatively quickly when the heat gun turns on, then rises nearly linearly after 400 s, reaching an amplitude of ±4.0 °C. The cell block temperature is approximately a triangle wave, rising or falling nearly linearly depending on the heat gun state, and has an amplitude of ± 1.8 °C. After 400 s, the cell air temperature and cell block temperature rise at the same rate. More importantly, the difference between the cell air temperature and the cell block temperature stabilizes at ±2.2 °C. This suggests the maximum error (difference between the cell block, which is measured, and the air sample in the cell, which is not measured) for the EC155 is 2.2/55 or 4%, even for very long periods.

The middle graph of Figure 1 shows the inlet air temperature still approximates a square wave, with similar amplitude to the very long period. The cell air temperature has a much smaller amplitude, and a very different shape. The temperature rises or falls nearly linearly depending on the heat gun state. The cell block temperature shows very little response, making the error almost indistinguishable from the cell air temperature.

The bottom graph of Figure 1 shows the inlet air temperature is more rounded and slightly delayed, with slightly smaller amplitude. The rounding and the delay result partly from the frequency response of the inlet air thermocouple's frequency response, and partly from the time required for the heat gun to turn on and warm up. The cell air temperature and the temperature error are noticeably delayed, with greatly reduced amplitude.

The FFT amplitudes (left) and phases (right) of the data are shown in Figure 2. The inlet air amplitude is flat over most of the frequency range, but drops slightly at the higher frequencies. The fine-wire thermocouple shows reduced amplitude and shifted phase at higher frequencies that are due to the heat gun warm-up time. The inlet air temperature shows a slight decrease in amplitude and phase shift compared to the fine-wire thermocouple that results from its somewhat reduced frequency response. The amplitudes for the cell air and cell block temperatures become progressively smaller at high frequencies, but reach a limit at approximately 0.002 °C. The error amplitude is distinguishable from the cell air only at the lowest frequency.

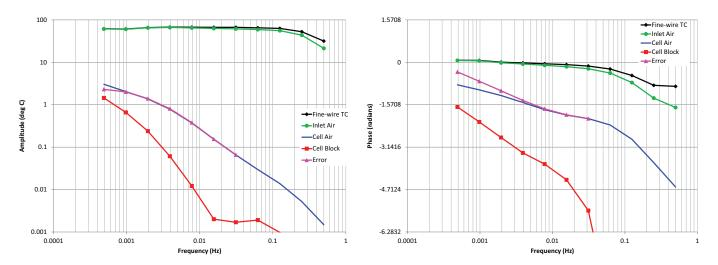


Figure 2. Complex temperature fluctuation spectra: Amplitude (left) and phase (right).

The phase of the inlet air and the fine-wire thermocouple is relatively flat at low frequency, but falls slightly at higher frequencies. This is consistent with the time delays associated with turning the heat gun on and the somewhat degraded frequency response of the inlet air thermocouple. The cell air phase falls in the low and middle frequencies, tending to be near -1.57 ($-\pi/2$) radians. This is consistent with a nearly linear rise/fall depending on the heat gun state. The phase of the cell block falls quickly, affecting the error phase over a wider range of frequencies than the amplitude.

Attenuation of temperature fluctuations in the EC155 intake tube was calculated by dividing the cell air by the inlet air. This damping ratio is shown as a complex spectral quantity in Figure 3. A closely related quantity, the relative error (temperature error divided by the inlet air), is also shown. The damping ratio amplitude is 0.05 at the lowest frequency measured (0.00049 Hz), falls to 0.01 at 0.005 Hz, and continues to fall at higher frequencies. The amplitude of the relative error is indistinguishable from the amplitude of the damping ratio at all but the lowest frequency. The relative error levels off at 0.04, while the damping ratio continues to rise at lower frequencies. This is consistent with the observation of the time series.

The phase of the damping ratio falls through the entire frequency range, but is relatively near -1.57 ($-\pi/2$) over much of the range. The phase of the relative error differs from the phase of the damping ratio more and more at lower frequencies.

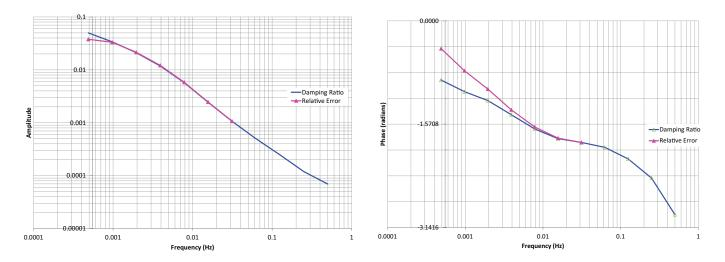


Figure 3. EC155 intake tube damping ratio and relative error: amplitude (left panel) and phase (right panel).

The damping ratio and the relative error presented in Figure 3 quantify how well the EC155 intake tube damps temperature fluctuations, and the error associated with measuring the cell block instead of the cell air. To characterize the effect of the small residual temperature fluctuations on an EC flux measurement, it is necessary to model the attenuation of the sensible heat flux (the WPL temperature term is proportional to sensible heat flux). The sensible heat flux is the integral of the cospectrum of temperature and vertical wind. This can be modeled for the air at the EC155 inlet and in the EC155 sample cell. The ratio gives an attenuation ratio.

The cospectral model is taken from Horstⁱ who proposed a simple model for the cospectrum that accounts for the change in spectral distribution with measurement height, wind speed, and atmospheric stability:

$$fCo(f) = \langle w'c' \rangle \left(\frac{2}{\pi}\right) \frac{f/f_m}{1 + (f/f_m)^2}$$

where:

Co(f) = the cospectrum of vertical wind speed and air temperature

f = frequency (Hz)

fCo(f) = the logarithmic cospectrum

 $\langle w'c' \rangle$ = the covariance of vertical wind (w) and a scalar c (air temperature)

 f_m = the frequency at which the function reaches its maximum

$$f_m = n_m \frac{\bar{u}}{z}$$

where:

 n_m = the normalized frequency of the logarithmic cospectral peak

 \bar{u} = mean horizontal wind speed

z = measurement height

The EC155 intake tube damps higher frequencies more effectively than lower frequencies. Therefore the model parameters were chosen to represent a worst case, as follows. The normalized peak frequency, n_m , depends on atmospheric stability. For this analysis it is assumed to be 0.085, the lower limit associated with neutral and unstable conditions. The quantity \bar{u}/z decreases at higher measurement heights, but tends to be on the order of one in most cases, because wind speed naturally tends to increase with height. For this analysis we have assumed \bar{u}/z ranges from 0.05 to 1.0. The lower limit could represent 2 m s⁻¹ wind speed at 40 m height, for example. Lower peak frequencies are unlikely to be of interest because data with a lower value of \bar{u}/z would most likely be discarded because of insufficient wind speed to develop turbulent transport. The upper limit could represent 2 m s⁻¹ wind speed at 2 m height, for example. Higher values of \bar{u}/z are not uncommon, so this represents typical value, not an upper limit. However, it is high enough to illustrate the variation.

Figure 4 shows the cospectral model for $\bar{u}/z = 0.05$, 0.1, 0.2, 0.5, and 1.0. These give f_m ranging from 0.004 to 0.085 Hz. All have the covariance $<\!w'c'\!>$ set to one. Following the usual convention, the logarithmic cospecturm fCo(f) is plotted to more clearly show the frequency range that contributes most of the flux.

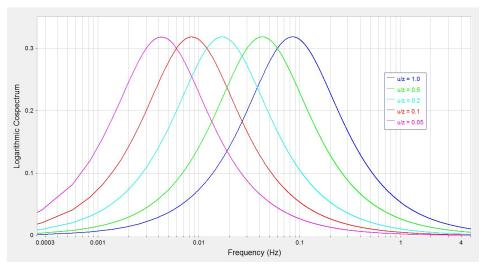


Figure 4. Modeled logarithmic cospectra for several values of \bar{u}/z .

Horst, T.W. 1997. "A simple formula for attenuation of eddy fluxes measured with first-order-response scalar sensors." *Boundary-Layer Meteorol.* 82, 219-233.

To model the sensible heat flux in the EC155 tube, the model cospectrum could be multiplied by the damping ratio. However, it is of more interest to use the relative error. This gives the error introduced by using the cell block temperature instead of the temperature of the air in the sample cell. As expected from the similarity of the damping ratio and the relative error, similar results are obtained if the damping ratio is used (data not shown).

The relative error has been presented using polar notation (amplitude and phase, Figure 3, left and right, respectively) but it is only the real part of the error (that part which is in phase with the vertical wind) that contributes to the sensible heat flux. The real part of the relative error is shown in Figure 5. This figure also shows the amplitude, for comparison. This graph shows the Y axis on a linear scale because the real part goes negative at approximately 0.007 Hz, where the phase passes through $-\pi/2$. The amplitude drops below 1% at 0.005 Hz, but the real part drops below 1% at 0.002 Hz, demonstrating the importance of the phase. The relative error measurements included data down to 0.00049 Hz (a period slightly longer than 30 minutes). This was extrapolated assuming an amplitude of 0.04 and a phase of 0 at 0 Hz to allow the model to include an additional datum at 0.00028 Hz (a one-hour period). It was then interpolated to the frequencies corresponding to the modeled cospectra.

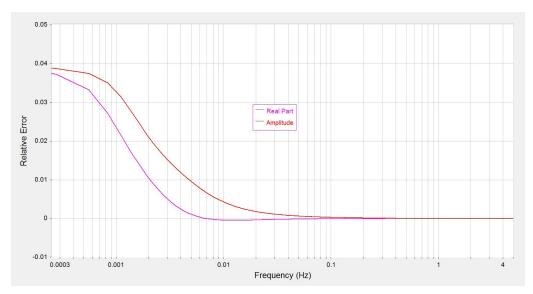


Figure 5. Real part of the relative error spectrum. Amplitude overlaid for comparison.

The modeled cospectra were multiplied by the real part of the relative error and integrated to give the residual error of the sensible heat flux. Ogive plots (cumulative integrals) are shown in Figure 6. The Ogives show that most of the flux is at frequencies below 0.002 Hz, where the relative error falls to 1%. Similar plots were generated using the amplitude of the relative error (data not shown). The residual sensible heat fluxes were approximately twice the actual values. The original cospectra models used a value of one for the sensible heat flux; therefore these figures show the relative residual error. The worst case ($\bar{u}/z = 0.05$) gives a value of 0.008, less than 1% of the sensible heat flux at the inlet.

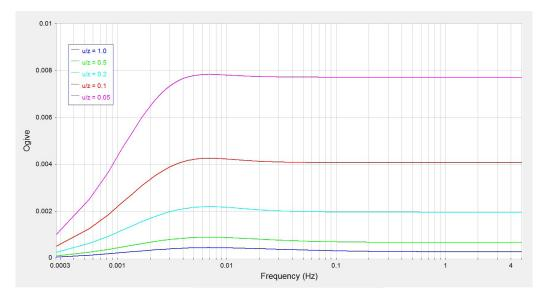


Figure 6. Ogives of residual sensible heat flux.

These results are plotted (as well as some additional values of \bar{u}/z) as a function of z/\bar{u} and shown in Figure 7. Plotting vs. z/\bar{u} instead of \bar{u}/z gives a nearly linear relationship, with a slope of 0.0004 as shown in Figure 7.

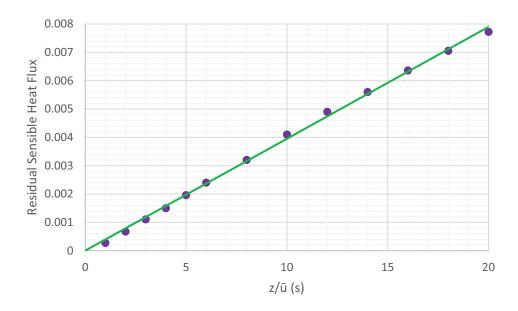


Figure 7. Residual sensible heat flux as a function of z/ū.

Summary

Rannik *et al.*^h used a simple steady-state model to provide a useful guideline for the length of tubing required to sufficiently damp temperature fluctuations so that a closed-path analyzer may ignore the WPL temperature term. That length is modeled to be 1000 times the diameter. They noted that fluctuations would damp more quickly than the steady state, and suggested the importance of experimental verification of physical intake tubes. At that time, commercial IRGAs with a very short intake tube that could be used for eddy covariance measurements, were unavailable. Recently developed field-rugged closed-path IRGAs, allow the use of very short intake tubes to help preserve the frequency response of the water vapor measurement. These new IRGAs motivated the present study to experimentally verify temperature damping in a very short intake tube.

One of the new IRGAs, the LI-7200, uses an intake tube that only partially damps temperature fluctuations. This IRGA includes fine-wire thermocouples at the inlet and outlet of the sample cell to measure the substantial residual fluctuations. Another of these IRGAs, the EC155, uses an integrated intake tube assembly designed to sufficiently damp temperature fluctuations to allow the use of a rugged thermocouple embedded in the sample cell block. This paper described a method for testing the damping ratio, and gave results for the EC155 intake tube assembly.

The EC155 temperature damping ratio was shown to increase strongly with frequency, as expected. The small residual temperature fluctuations tended to be out of phase with the temperature fluctuation at the inlet, further reducing the effect. Very low frequency fluctuations were partly measured by the thermocouple in the sample cell block. Modeling the attenuation of the WPL temperature term took into account the residual error (the difference between the cell block temperature and the temperature of the air in the sample cell). This residual error was plotted as a complex function of frequency and was applied to cospectral models to show that the temperature fluctuations are sufficiently damped that it is not necessary to measure the temperature of the air in the sample cell. Residual sensible heat flux (error) is less than 1% of the original, even for extreme worst-case conditions: high measurement heights and low wind speeds where there is significant flux at low frequencies.

